MNRAS **000**, 1–7 (2019) Preprint 7 July 2019 Compiled using MNRAS LATEX style file v3.0

The Grand Twirl: the epoch of rapid assembly of extended disc galaxies

Person,[1]★ A. N. Other,[2] Third Author[2,3] and Fourth Author[3]
[1]*Royal Astronomical Society, Burlington House, Piccadilly, London W1J 0BQ, UK*
[2]*Department, Institution, Street Address, City Postal Code, Country*
[3]*Another Department, Different Institution, Street Address, City Postal Code, Country*

Accepted XXX. Received YYY; in original form ZZZ

ABSTRACT

Galactic outflows driven by stellar feedback are crucial for explaining the inefficiency of galaxy formation. Although strong feedback can promote the formation of galactic discs by removing low angular momentum gas, it is still not understood how the same feedback can result in the thin, kinematically cold discs we observe today. In this work we investigate this problem using cosmological zoom simulations of two galaxies forming in 10^{12} $M_\odot$ haloes with almost identical mass growth histories. After a starburst episode triggered by the last major merger at $z \sim 1.5$, the galaxies' similar evolutionary paths diverge, with one galaxy ending up as a compact elliptical, whereas the other as an extended star forming disc. The origins of this behaviour is the angular momentum of accreted gas, and whether it adds *constructively* to disc formation. At $z > 1.5$, both galaxies feature a surface density of star formation $\Sigma_{\rm SFR} \sim 10\ M_\odot\ {\rm yr}^{-1}\ {\rm kpc}^{-2}$. Post starburst, the disc rapidly grows in size, leading to $\Sigma_{\rm SFR} < 0.1\ M_\odot\ {\rm yr}^{-1}\ {\rm kpc}^{-2}$ hence spreading out the effect of supernova feedback and the formation of a thin extended disc. BLABLABLA **OA: Something on the fact that extended disc formation, and lower gas fractions, lead to the star formation surface density dropping below "the critical value" at late times –> thin discs.**

Key words: keyword1 – keyword2 – keyword3

1 INTRODUCTION

We have made incredible advances in understaning the physics of our universe (Newton 1687; Einstein 1916; Kretschmer & Teyssier 2019). Most stars form in $L_\star$ galaxies. with only a few percent of the cosmic baryon fraction ending up as stars in Milky Way mass halos ($M_{\rm halo} \sim 10^{12}\ M_\odot$), on average. Mass loading is known to decrease with galaxy mass. However, how galaxies transition between an outflow driven evolution at $z > 1$, to settling into large and thin galactic discs, seemingly undisturbed by vigorous feedback, is not yet understood. Empirically, this transition is found to be rapid (~ 100s of Myr), hence posing a challenge for galaxy formation models.

2 METHODS

2.1 numerical setup

We now report on the numerical experiment we have performed. We model the cosmological evolution of two dark matter halo, whose mass is comparable to the Milky Way mass and whose accretion history is similar. In particular, we choose two halos without major mergers after expansion factor $a > 0.5$. With this we can investigate the formation of two similar halos although they will result in very different galaxies at $z = 0$. As it turns out, this particular halos feature a strong starburst at $a = 0.?$ and $a = ??$ respectively, followed by an quiescent state. We identify one resulting galaxy as a typical example of the population of early-type galaxies and the other one as a typical example of the population of a spiral S0-type galaxy.

We base our analysis on two cosmological zoom-in simulations that were performed with the AMR code RAMSES (Teyssier 2002). The two halos were selected in a dark-matter-only run and particularly selected to have very similar mass accretion history. The virial mass at $z = 0$ are

Both halos have no major merger after $z = 1$. The halos were run again with gas inserted. The minimum gas cell size is $\Delta x_{\rm min} = 55 - 110$pc.

★ E-mail: mn@ras.org.uk (KTS)

2.2 Simulation setup

We base our analysis on a cosmological zoom-in simulation that we performed with the AMR code RAMSES (Teyssier 2002). We first ran a reference pure N-body simulation with 512^3 particles in a periodic box of size 25 h^{-1}Mpc. We selected two halos at redshift 0 of virial mass $M_{\rm vir} = 1.1 \times 10^{12} {\rm M}_\odot$ and $M_{\rm vir} = 1.4 \times 10^{12} {\rm M}_\odot$ in an isolated environment. Here the virial mass is calculated using a spherical overdensity, according to the criterion of (Bryan & Norman 1998). I have to redo all the plots for this definition.

We then generated new initial conditions around these halos with the MUSIC code (Hahn & Abel 2011), with an initial hierarchy of concentric grids from $\ell_{\rm min} = 7$, corresponding to a coarse grid resolution of 128^3 covering the entire periodic box, to $\ell_{\rm max,ini} = 11$, corresponding to an effective initial resolution of 2048^3. This gives us a dark matter particle mass of $m_{\rm dm} = X.X \times 10^X {\rm M}_\odot$ and a baryonic initial mass resolution of $m_{\rm dm} = X.X \times 10^X {\rm M}_\odot$. We then performed simulations including gas and galaxy formation physics. The maximum resolution was set to $\ell_{\rm max} = 19$ at $z = 0$, while refinement levels were progressively released to enforced a constant physical resolution of $\Delta x_{\rm min} = 55$pc. The adopted refinement criterion is the traditional quasi-Lagrangian approach, namely cells are individually refined when more than 8 dark matter particles are present or when the baryonic mass (gas and stars) exceed $8 \times m_{\rm bar}$. Only the Lagrangian volume corresponding to twice the final virial radius of the halo was refined, the rest of the box being kept at a fixed, coarser resolution to provide the proper tidal field. Our zoom simulations at $z = 0$ correspond to Milky Way-like halos. The major merger events at a =? and z =? have stellar mass ratios of $X : X$ where the stellar mass of each galaxy was $M_* \simeq X.X \times 10^9 {\rm M}_\odot$

Additional detailed information of standard physical models that we use in RAMSES can be found in (Kretschmer & Teyssier 2019).

The RAMSES settings for these 3 simulations are as follows. We used the HLLC Riemann solver, modified to account for the supernovae dynamical pressure. The star particle was set equal to the baryonic mass resolution $m_* = m_{\rm bar}$. We adopted the *MinMod* slope limiter, an important choice to ensure the stability of the new feedback scheme. The adiabatic exponent of the gas was set to $\gamma = 5/3$. We didn't use any polytropic pressure floor, as our star formation model, by construction, very quickly removes gas for which the Jeans length is not resolved. The gas metallicity was initialised to $Z_{\rm ini} = 10^{-3} Z_\odot$ to account for early population III stars enrichment.

2.3 subgrid physics for SF and FB

The model for starformation is the same *multi-freefall* model as discussed in (Kretschmer & Teyssier 2019). This star formation model is based on a subgrid turbulence model, and provides a varying star formation efficiency that depends on the local conditions in each computational cell, through the cell's virial parameter and its turbulent Mach number. The density distribution of gas in a turbulent medium is given by a log-normal PDF $p(s)$ with mean $s = \ln \rho/\rho_0$ and variance σ_s with a density ρ and mean density ρ_0. A part above a critical density $s_{\rm crit}$ of the gas-PDF should form stars. Therefore, the starformation rate per free fall time ${\rm SFR}_{\rm ff}$ is obtained by integrating the PDF weighted by the densities and free-fall above $s_{\rm crit}$ (Hennebelle & Chabrier 2011; Federrath & Klessen 2012):

$$\begin{aligned} {\rm SFR}_{\rm ff} &= \frac{\epsilon}{\phi_t} \int_{s_{\rm crit}}^{\infty} \frac{t_{\rm ff}(\rho_0)}{t_{\rm ff}(\rho)} \frac{\rho}{\rho_0} p(s)\, {\rm d}s \\ &= \frac{\epsilon}{2\phi_t} \exp\left(\frac{3}{8}\sigma_s^2\right) \left[1 + {\rm erf}\left(\frac{\sigma_s^2 - s_{\rm crit}}{\sqrt{2\sigma_s^2}}\right)\right] \end{aligned} \quad (1)$$

have to change this stuff below... We set the prefactors $\epsilon/\phi_t = 1$ such that the ${\rm SFR}_{\rm ff}$ is given by the integrated PDF without further fudging.

We adopt the approach of Krumholz & McKee (2005), where $s_{\rm crit}$ is estimated by comparing the Jeans length λ_J at the mean density with the sonic scale λ_s. The sonic scale is the lower end of the turbulent cascade, where turbulence becomes subsonic and therefore cannot produce subfragmentation. At this scale, the thermal pressure becomes similar to the turbulent pressure and the Jeans criterion can be applied (Vázquez-Semadeni et al. 2003):

$$s_{\rm crit,KM} = 2 \ln\left(\phi_x \frac{\lambda_J}{\lambda_s}\right) = \ln\left[(\pi^2/5)\phi_x^2 \alpha_{\rm vir} \mathcal{M}^2\right] \quad (2)$$

with the Mach-number $\mathcal{M} = \sigma_v/c_s$, a numerical fudge-factor $\phi_x = 1.12$ taken from (Krumholz & McKee 2005) and the virial parameter:

$$\alpha_{\rm vir} = 2E_{\rm kin}/|E_{\rm grav}| \quad (3)$$

which measures the ratio of kinetic to gravitational energy of a given clump. Namely a bound object has $\alpha_{\rm vir} < 1$ and should contract and is hence expected to form stars.

Feedback is implemented as thermal and momentum feedback from supernovae, where the values obtained by Martizzi et al. (2015) for an 'in-homogeneous medium' are used. Additionally we enable photo-ionization in H_{II} regions.

3 RESULTS

3.1 "describe the 'critical merger' event:"

Both halos have a similar mass growth history that result in MW-like halos at $z = 0$. The baryon fractions that reside in them is actually its quit high... Also the galaxies that form in these halos will have stellar masses in line with the Milky Way.

The galaxies undergo a sequence of starbursts up to $z \sim 1.5$ where a last strong star burst is triggered by a merger. Both halos have similar accretion history, in the sense that both of them experience the last merger before $z > 1.5$ such that both have potentially enough time to form extended disks.

Figure 1 shows the evolution of SFR and the effective radius (half-mass radius) of the cold-gas disk inside $0.1R_{\rm vir}$ as well as the in- and outflows that were measure through a shell at $0.5R_{\rm vir}$ of thickness $\Delta r = \pm 0.3 R_{\rm vir}$. The dashed lines indicate the moment of the last starbursts in each galaxy. For both galaxies, it is apparent that shortly before the starburst, there is a small peak in the inflow $\dot{M}_{\rm in}$ which is the infalling merger. The merger will cause gas to be pushed to large densities and large turbulent velocity dispersions. This

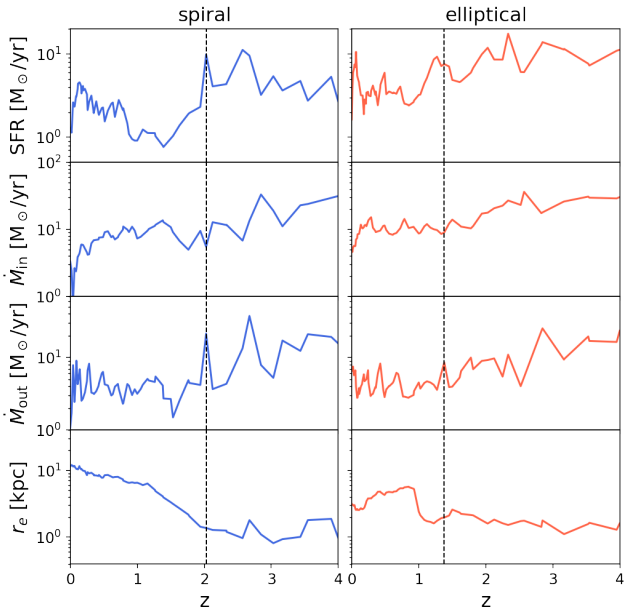

Figure 1. AM vs scalefactor

will result in very high star formation efficiencies and consequently a peak in SFR, namely a starburst (dashed vertical lines), which is visible in the first row of Figure 1. The consequence of this starburst is that shortly after a fraction of the newly formed stars will explode in supernova.

These spatially clustered events put large amount of energy in the surrounding gas and effectively remove it from the galaxy by pushing it outwards. Figure 2 shows strong outflows following the last starbursts in one of the galaxies. Gas is moving with high radial velocities from the center outwards. Much of the gas will leave the halo and never fall back A2. Most of the pushed gas is heated to high temperatures of $T \gtrsim 10^6$ K and relatively low surface density.

These violent star burst events are crucial to regulate the baryonic content of the halos. Namely, they set the amount of gas in the halo that will be left in the cold dense disk to form stars or stay in the hot, dilute halo phase. Consequently, feedback must be strong enough to remove a good amount of baryons from the halo such that at z=0 we get the right baryon fraction. **Oscar: at the same time, the same strong feedback can easily destroy the disc, leading only to nonphysically thick discs (see Roškar et al. (2014)). What actually happens, and this is impart supported observational, is that feedback activity slows down as Σ_{SFR} decreases. We find that this is not a gradual process, but a rapid transition after the final starburst.** The outflows $\dot{M}_{out}$ are also visible in Figure 1.

Shortly after this event the SFR decreases in both galaxies, because the star forming gas is consumed and the rest of the gas is left in a state where star formation is not possible.

Interestingly we see that immediately after, the effective radius quickly increases. We see that an extended disk is formed from co-rotating merger debris and satellite material (cold and dense gas - it seems that this is not cooled halo-gas.) **O: this is a very rapid event. The gas disc quickly forms, and a stellar disc then builds up over many Gyrs** Namely, a thin disk of dense gas is rapidly formed, mainly of the debris from the merger event.

We will discuss the formation of the disk in detail below. This sequence of a merger driven compaction into a compact object, followed by a star burst and finally the growth of an extended disk is known as compaction (Zolotov et al. 2015; Dekel et al. 2019).

we could add eccentricity distribution plots of the stars befor or shortly after the merger. then we also make the same but at z=0 to show the transition from a thick to a thin disk. or just a surface density plot and compare it to Figure 4.

todo before: a messy and perturbed gas disk. thick stellar disk with high dispersion

3.2 "build up of the disk and survival/late evolution"

We will now focus on the build up and survival of the gas disk and it's late evolution. As described above, both galaxies rapidly form gas disks after their last starburst. Up to this point both galaxies are very similar. However, afterwards their evolution becomes very different. Figure 4 shows projections of the gas and star distribution at $z = 0$. Clearly one galaxy forms an extended gas disk where the other forms a small disk and lots of halo-gas. The first galaxy forms a large stellar disk with a thick and a thin component where the other forms a compact elliptical stellar system. The first simulated galaxy can be identified as a typical example of the population of early-type galaxies and the other one as a typical example of the population of a spiral S0-type galaxy.

The angular momentum vector J is computed by considering all stars i within $0.1R_{vir}$:

$$J = \sum_i m_i (r_i \times v_i) \tag{4}$$

and the (z-component of the) specific angular momentum (sAM) is $j_\star = J_z/M_\star$.

In Figure 3 we show the evolution of the specific angular momentum of the stars $j_\star$ of the two galaxies as a function of their stellar mass. It is apparent that up to the point of the last starburst (which is highlighted as a small circle) the evolution of the two galaxies is very similar. In detail, $j_\star$ is increasing with the stellar mass of the system. After the last starburst the evolutionary tracks diverge such that for one galaxy $j_\star$ is increasing by an order of magnitude into the regime of observed spiral galaxies. The other galaxy however looses a lot of $j_\star$ (up to an order of magnitude) and finally ends up in the observational regime of elliptical galaxies. The classification of $j_\star$ vs $M_\star$ as elliptical or spiral is clearly in agreement with the visual images that we show in Figure 4.

To understand the origin of the diverging evolutionary tracks we look at the angular momentum J of cold gas ($T < 5 \times 10^4$K) no density cut inside the virial radius. Figure 5 shows face-on maps of J at different redshifts for both galaxies, where the orientation of the galaxy was computed by using the cold gas inisde $0.1R_vir$. At high redshift ($z \simeq 2.5$) both galaxies show lots of cold gas mass counter- and co-rotating. However going forward in time, it is apparent that for the first galaxy most of the cold gas is co-rotating. We see co-rotating cold gas streams that reach from the halo and

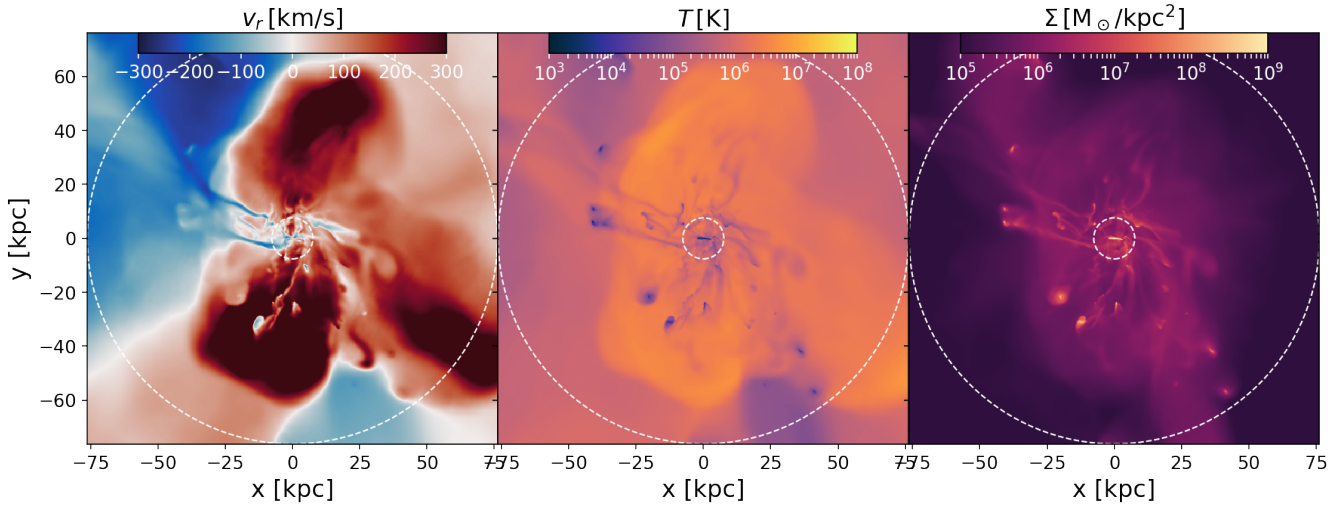

Figure 2. Strong outflows that follow the last starburst. Plots from left to right show projected mass-weighted radial velocity v_r, temperature T and density Σ. Dashed circles indicate $0.1R_{\rm vir}$(inner) and $1.0R_{\rm vir}$ (outer). The Plots show that lots of dense and hot gas is pushed outwards with large velocities.

merge with the cold galactic disc. The size of the galactic disc is steadily increasing with time. In contrast to this, the halo of the second galaxy is filled with lots of counter-rotating cold gas that is also coming from the halo and merging with the disk. This negative angular momentum gas is slowly diminishing the galactic disk, until there is only a tiny cold gas disk left with a counter-rotating core.

The origin clearly is that in one case accreted gas adds constructively to disc formation and in the other it's not.

text ...

However only one is able to sustain/expand the disk to z=0. (This is because of the positive AM accretion.) Here we can comment on the (Sales et al. 2012) idea. Mike Fall' work on angular momentum Scannapieco Aquila project Tim Heckman's work on SigmaSFR. Patch models of outflows: Ostriker work, Walch et al.? Evan Scannapieco work. Shy Genel on ang mom in Illustris. Work by Dolag et al. on Magneticum sim (ang mom) New Horizon work: discs vs early types. Hanna Ubler (w. Naab. Feedback promotes disc formation due to ang mom business. Pre-grand twirl history in terms of outflows. 0)

Galactic bifurcation: disc formation triggers end of feedback dominated regime. Low angular momentum case is a channel for quenching via (rapid?) self depletion. But, lack of AGN makes this difficult.

Lehnert: the SigmaSFR derived by Lehnert et al. is for solar neighbourhood stars, derived from stellar chemistry arguments. (Oscar to add)

? Greg Bryan work on overdoing outflows -> too large discs (fine-tuning?)

Hubble sequence stuff: astro botanics or astro ecology. Flora and fauna of galaxies. Galactic biodiversity. Galaxy formation in the green energy era.

3.3 Evolution of starformation intensity

We now show the evolution of the surface star formation rate (or SFI for star formation intensity) in both galaxies.

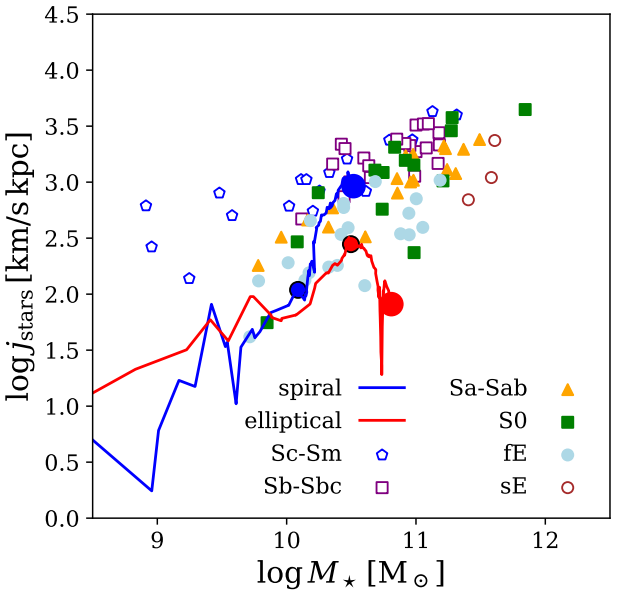

Figure 3. Evolution of the specific angular momentum of the stars for the two galaxies as a function of their stellar mass. Blue is the galaxy that will end up as a sprial at z=0 and red is the elliptical. The small circle in the same color of the line is the moment of the last star burst. The big circle is the point at z=0. Data points are taken from (Fall & Romanowsky 2013) where circles are ellipticals and others are spirals.

The surface star formation rate is defined as

$$\Sigma_{\rm SFR} = \frac{\rm SFR}{\pi r^2_{\rm SFR/2}}, \quad (5)$$

where $r_{\rm SFR/2}$ is the half-SFR-radius. should there be a 2 ? Lehnert uses SFR/$2\pi r_d^2$ where r_d is the scale length of the disk. Also in 'paper 1' we define it as SFR/$2\pi r_h^2$ with r_h the

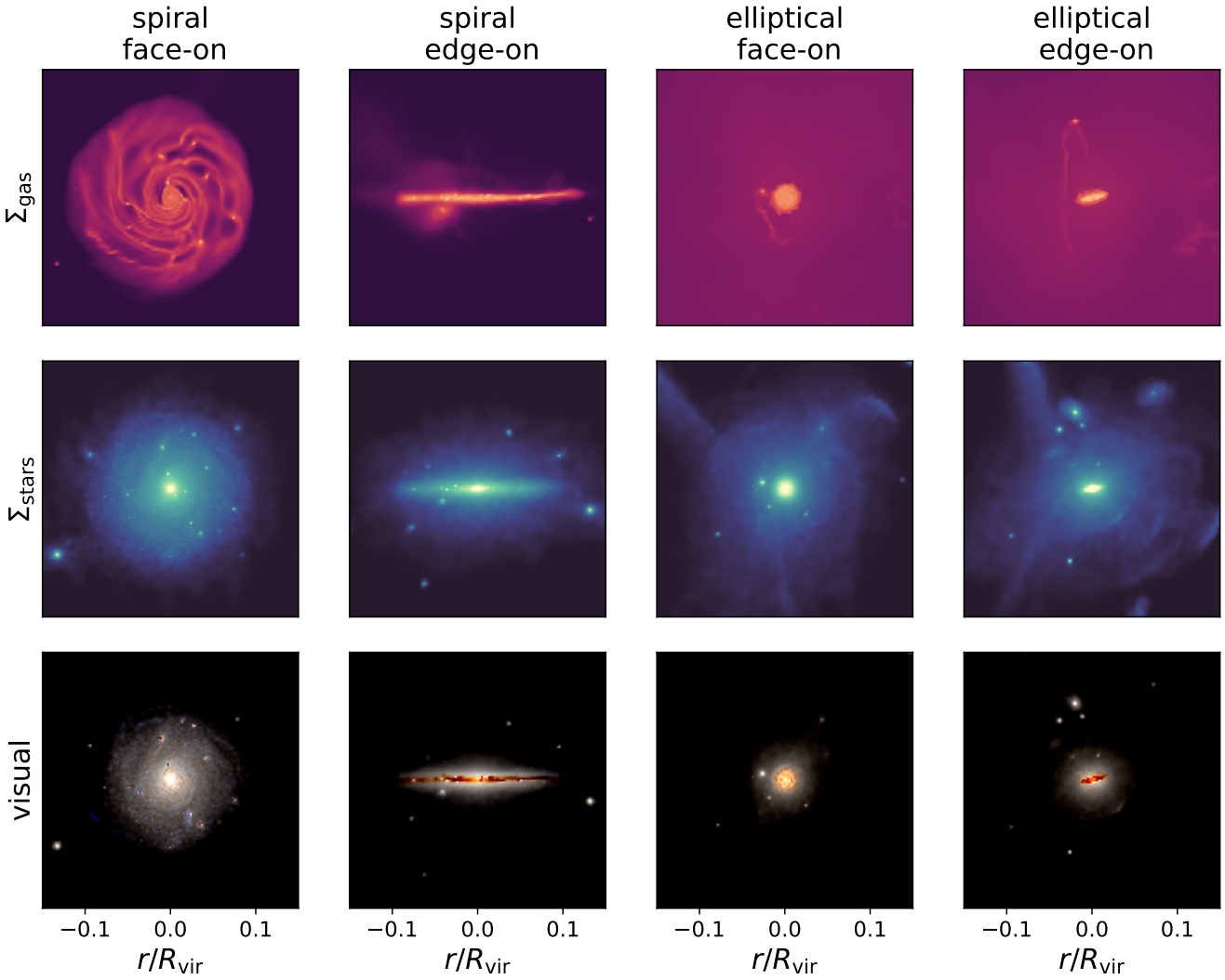

Figure 4. some visuals ... all at $z = 0$, left:nice galaxy, right: bad elliptical. from top to bottom: gas, stars, render. (Render could be redone in better RGB channels. colorbars, units, ...) maybe redo with `gridspec`

half-mass-radius of the cold gas.. In Figure 6 we show the evolution of $\Sigma_{\rm SFR}$ for both galaxies as a function of redshift and compare it to results for the Milky Way obtained by Lehnert et al. (2014). At high redshift both galaxies have high SFI with $\Sigma_{\rm SFR} \sim 10\,{\rm M}_\odot{\rm yr}^{-1}{\rm kpc}^{-2}$, which is maintained until $z \sim 1.5$. As discussed earlier, until here the evolution of the two galaxies is very similar. After this point however, the SFI in one galaxy (the spiral galaxy) drops very rapidly to a value of $\Sigma_{\rm SFR} < 0.1\,{\rm M}_\odot{\rm yr}^{-1}{\rm kpc}^{-2}$ wheraes the other galaxy maintains a high SFI until $z = 0$. The fast drop in SFI can be explained by the rapid disk growth of this galaxy, decreasing $\Sigma_{\rm SFR}$ with $\propto r_{\rm SFR/2}^{-2}$. This evolution is in perfect agreement with results for the Milky Way obtained by Lehnert & Heckman (1996). Interestingly we see that the SFI drops below a value of $\Sigma_{\rm SFR} = 0.1\,{\rm M}_\odot{\rm yr}^{-1}{\rm kpc}^{-2}$ which has been identified in local galaxies as a threshold for starburst-driven outflows (Lehnert & Heckman 1996; Heckman 2003). From Figure 1 we see that indeed outflows are very weak after the formation of the disk $z < 1.5$ but on the other hand were occasionally strong at high redshift ($\dot{M}_{\rm out} > 10{\rm M}_\odot{\rm yr}^{-1}$. but the elliptical also does that....

To investigate this further we focus on radial profiles of $\Sigma_{\rm SFR}$ shown in Figure 7. First we discuss the radial profiles normalized to $0.1R_{\rm vir}$ (top panels). For the spiral galaxy we find that $\Sigma_{\rm SFR}(r)$ evolves from high everywhere to small in the disk and slightly larger in the bulge. Namely at high redshift, the starformation intensity is large enough to cause starburst-driven outflows, which is also seen by comparing to the typical threshold-value. With time, an extended disk is formed and the SFI decreases. Only in the bulge, where SF is proceeding at a slightly larger level SFI is slightly larger. However at $z = 0$, $\Sigma_{\rm SFR}$ in the whole disk is too small to cause outflows, explaining the emergence of a quiescent disk. Additionally we see, that $\Sigma_{\rm SFR}(r/0.1R_{\rm vir})$ stays constant in time which was highlighted before e.g. in Kravtsov (2013).

In the case of the elliptical there is no build up of a star forming disk, but instead star formation is only happening in a compact central region. Clearly this is explained by the above mentioned failed build up of an extended cold gas

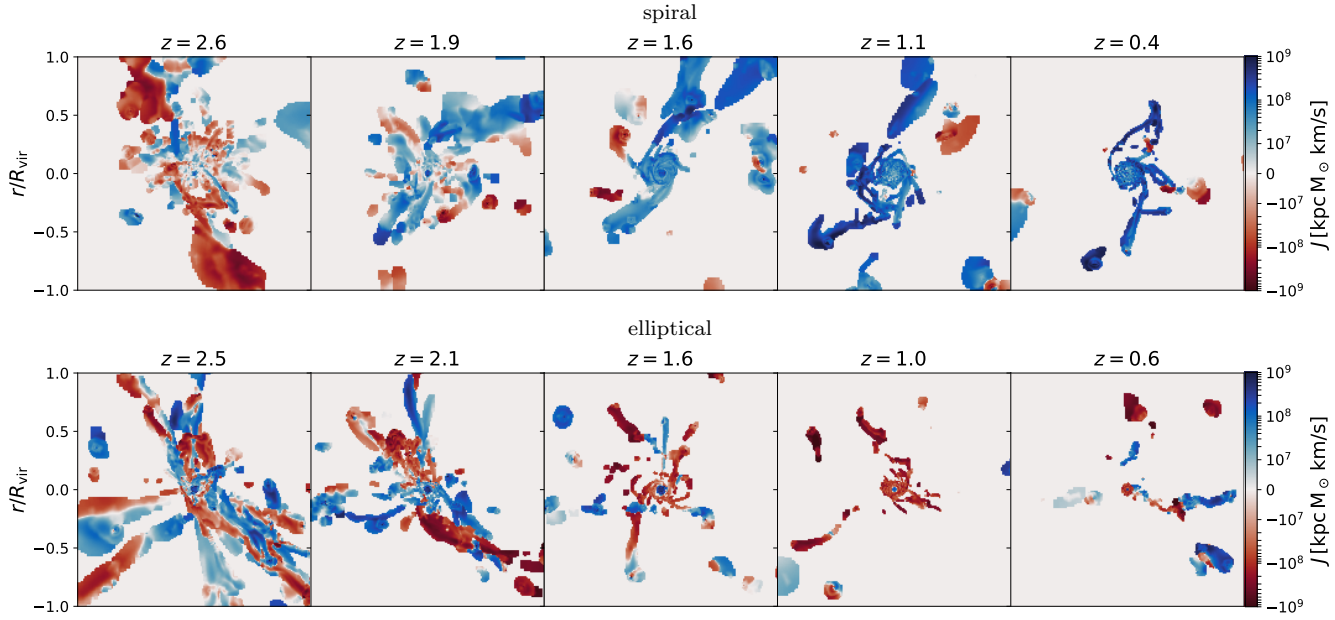

Figure 5. top: nice galaxy (spiral). bottom: elliptical. Plots are $z \sim 2.5, 2.0, 1.5, 1.0, 0.5$. Have to add labels, maybe circles for rvir and 0.1 rvir etc... Red means counter-rotating. Blue means co-rotating.

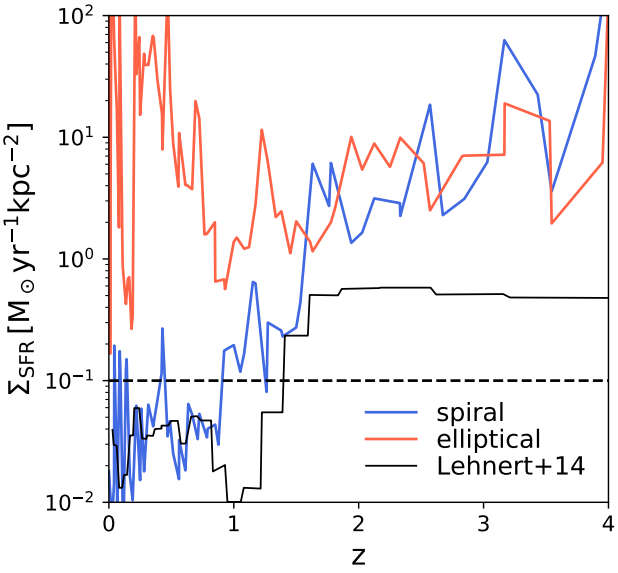

Figure 6. like (Lehnert et al. 2014)

disk. The $\Sigma_{\rm SFR}$ remains large over time which causes high turbulence and hindering the emergence of a quiet disk.

Looking at the radial profiles as a function of physical size (bottom panels), we see for the spiral the build up of an extended disk with low SFI. For the elliptical galaxy, $\Sigma_{\rm SFR}(r)$ stays constant in time, namely the physical size is unchanged.

4 DISCUSSION

text ...

5 CONCLUSIONS

(i) Disc building is quite rapid! A few 100s of Myr is what it takes to increase $r_1/2$ by a factor of >2.

(ii) Point 1 happens after the last star burst. In case of deconstructive accretion, the opposite happens

(iii) The stellar disc then slowly builds up, in agreement with e.g. van dokkums papers (check out Mstar vs r in his 3D-HST papers)

(iv) This 'transition' leads to a SHARP decrease in $\Sigma_S FR$, as is thought to be the case for the MW.

(v) Point 4 explains why thin discs can co-exist with the notion of strong feedback, i.e. strong feedback is only destructive for $\Sigma_S FR > 0.1$ (or so)

(vi) Bonus point: feedback models not agreeing with point 4-5 are likely incorrect.

ACKNOWLEDGEMENTS

Thanks.

REFERENCES

Bryan G. L., Norman M. L., 1998, ApJ, 495, 80
Dekel A., Lapiner S., Kretschmer M., Tacchella S., Ceverino D., Primack J., 2019, in prep., 01, 1
Einstein A., 1916, Ann. Phys., 354, 769
Fall S. M., Romanowsky A. J., 2013, ApJ, 769, L26
Federrath C., Klessen R. S., 2012, ApJ, 761, 156
Hahn O., Abel T., 2011, MNRAS, 415, 2101

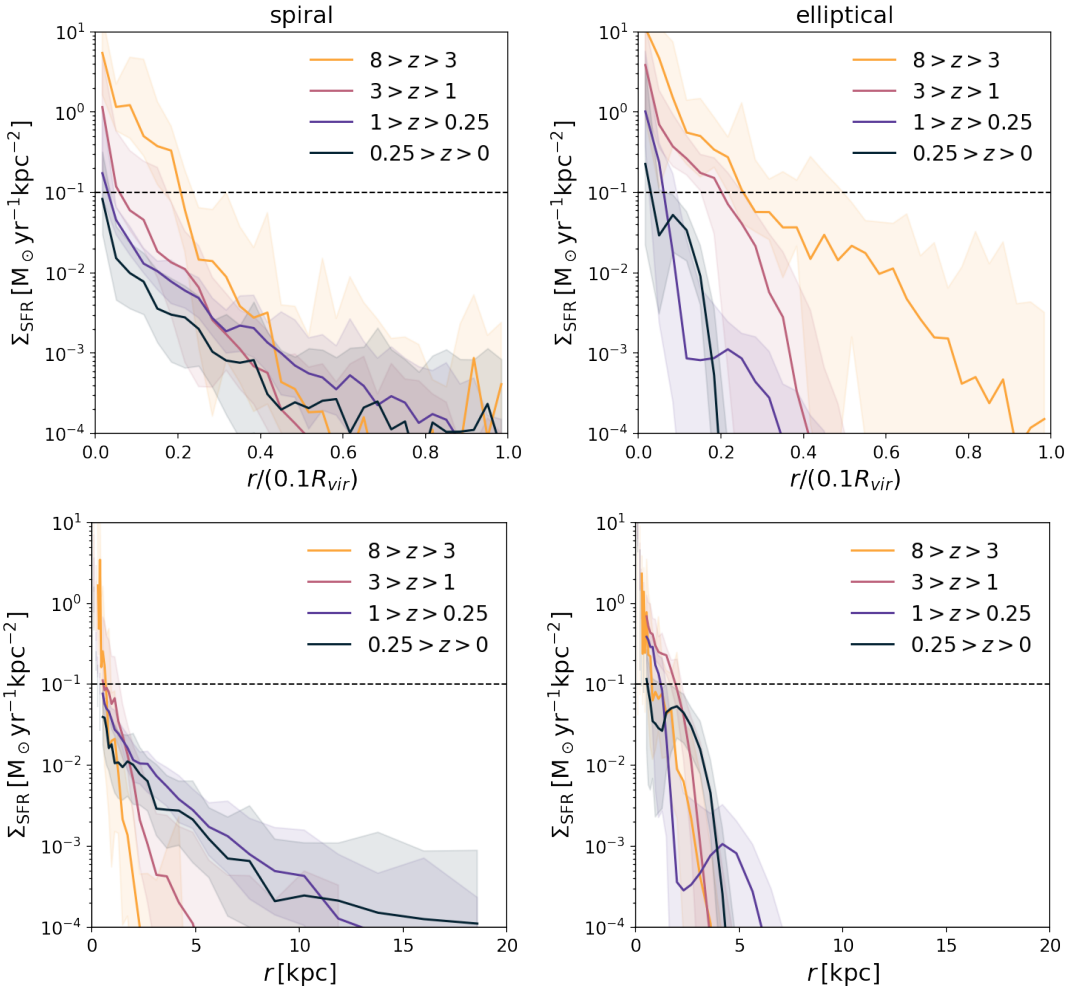

Figure 7. left: spiral, right: elliptical. top: normalised to $0.1R_{\rm vir}$, bottom: physical kpc.

Heckman T., 2003, in Avila-Reese V., Firmani C., Frenk C. S., Allen C., eds, Revista Mexicana de Astronomia y Astrofisica Conference Series Vol. 17, Rev. Mex. Astron. y Astrofis. Conf. Ser.. pp 47–55

Hennebelle P., Chabrier G., 2011, Astrophys. J. Lett., 743

Kravtsov A. V., 2013, Astrophys. J. Lett., 764

Kretschmer M., Teyssier R., 2019, arXiv e-prints, p. arXiv:1906.11836

Krumholz M. R., McKee C. F., 2005, ApJ

Lehnert M. D., Heckman T. M., 1996, ApJ, 472, 546

Lehnert M. D., Di Matteo P., Haywood M., Snaith O. N., 2014, Astrophys. J. Lett., 789, 1

Martizzi D., Faucher-giguère C. A., Quataert E., 2015, MNRAS, 450, 504

Newton I., 1687, Philosophiae naturalis principia mathematica. J. Societatis Regiae ac Typis J. Streater, https://books.google.ch/books?id=-dVKAQAAIAAJ

Roškar R., Teyssier R., Agertz O., Wetzstein M., Moore B., 2014, MNRAS, 444, 2837

Sales L. V., Navarro J. F., Theuns T., Schaye J., White S. D., Frenk C. S., Crain R. A., Dalla Vecchia C., 2012, MNRAS, 423, 1544

Teyssier R., 2002, Astron. Astrophys., 385, 337

Vázquez-Semadeni E., Ballesteros-Paredes J., Klessen R. S., 2003, ApJ, 585, L131

Zolotov A., et al., 2015, MNRAS, 450, 2327

APPENDIX A: SOME EXTRA MATERIAL

Stuff that I didnt do:

- spin parameter for hot/cold gas separately
- mass-loading factor
- gas-mass in fixed shells 10 ... 100 kpc

This paper has been typeset from a TEX/LATEX file prepared by the author.

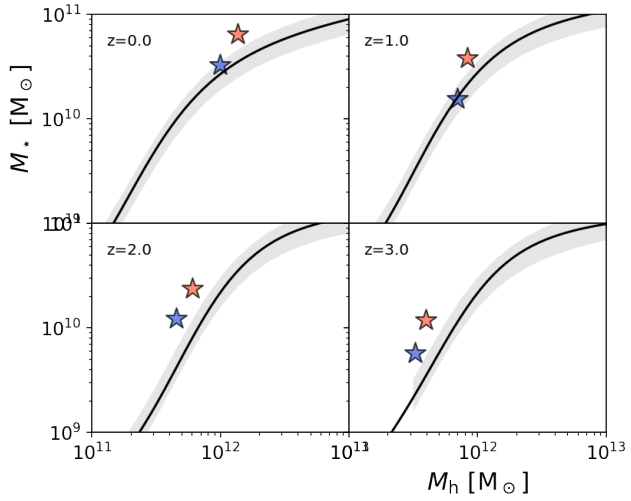

Figure A1. abundance matching

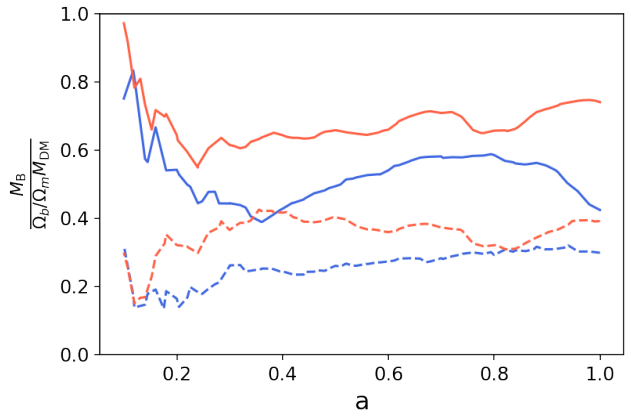

Figure A2. baryon fraction. dashed is inside 0.1 rvir.